

# Numerical Investigation of the Cross-section and Twist Extrusion Die Angle on the Distribution of Plastic Strain and Microstructure of Al7050 Alloy

F. Heydari, H. Saljoghi, S.H. Nourbakhsh\*

Mechanical Engineering Department, Shahrekord University, Shahrekord, Iran.

## Article info

### Article history:

Received 31 August 2019

Received in revised form

01 November 2019

Accepted 30 December 2019

### Keywords:

Twist extrusion

Die angle

Cross-section

Severe plastic deformation

Microstructure

## Abstract

Twist extrusion is a novel method for severe plastic deformation of materials. Severe plastic deformation in metals creates small and uniform grain size and therefore increases their mechanical strength. In this study, the effect of die angle in twist extrusion and cross-section of extruded parts on plastic properties and microstructures of Aluminum 7050 alloy was investigated using DEFORM 3D finite element software. Samples were simulated using dies with die angles of 20, 37, and 56 degrees with square, rounded-rectangular, and elliptical cross-sections. The aspect ratios of rectangular and elliptical cross-sections were also changed while keeping the cross-section area constant in order to investigate the effects of dimensions. Plastic strain distribution, grain size distribution, and the force needed for extrusion were extracted under all conditions. The results indicate that increase in die angle significantly reduces grain size and increases the force necessary for extrusion. Removing sharp corners in cross-section also results in more uniform plastic strain distribution and reduction in extrusion force. The elliptical cross-section with dimensions of  $9 \times 6$  mm which had the lowest dimension ratio can reduce grain size from 100  $\mu$ m to 6  $\mu$ m in a single pass and requires the lowest extrusion force.

## Nomenclature

$X$	Twist angle	$Q$	Activation energy
$L$	Length	$R$	Universal gas constant
$\beta$	Die angle	$T$	Absolute temperature
$\sigma^p$	Peak stress	$X$	Dynamic recrystallisation fraction
$\dot{\epsilon}$	Strain rate	$\epsilon_{0.5}$	Strain for 50% recrystallization
$d_0$	Initial grain size		

## 1. Introduction

Severe plastic deformations have been accepted in recent years as strong methods for improving the mechanical properties of metal parts. Using these processes, it is possible to create microstructures with ul-

trafine grains or even nanosized grains. These fine-grain materials can have higher strength and elongation [1]. Examples of severe plastic deformation include ECAP [2], Twist extrusion [3], Friction stir process [4], ARB [5], HPT [6], etc. Twist extrusion is one of the most common methods for creating severe plastic de-

\*Corresponding author: S.H. Nourbakhsh (Assistant Professor)

E-mail address: [nourbakhsh.sh@eng.sku.ac.ir](mailto:nourbakhsh.sh@eng.sku.ac.ir)

<http://dx.doi.org/10.22084/jrstan.2019.19974.1106>

ISSN: 2588-2597

formations. Twist extrusion uses a die made of two direct channels which are separated by a channel known as twist channel (Fig. 1). This twist channel is characterized using its twist angle  $x$ , length  $L$ , and radius  $R$ . One of the important geometrical properties used to describe twist channel is the angle between its axis and a line tangent to the extrusion channel spiral. This angle, is known as a die angle and is calculated using the equation  $\tan \beta = \frac{xR}{L}$  based on other geometrical properties.

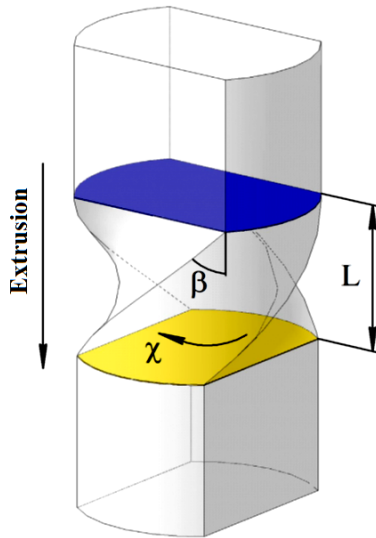


**Fig. 1.** Schematics of twist extrusion die [3].

The values selected for different dimensions of the die affect the accumulated plastic strain. On average, each two passes of the process create a plastic strain around 1.2 [6]. Since the cross-section area of the part remains constant during this process, it is possible to achieve high accumulated plastic strains using several passes of the process. To this day, several studies have investigated twist extrusion using finite element analysis [7-10] as well as theoretical and empirical methods [11-15]. Jahedi et al. [7] in 2011 used simulation to investigate the effects of friction and process speed on the accumulated plastic strain created in the extruded samples. Their results showed that the highest strain was observed in the corners and the lowest strain was present at the center of the part. The strain value also varied between 0.3 and 1.3. Another study by Akbari Mousavi et al. [8] used ABAQUS software to investigate the effect of temperature and strain rate in the twist extrusion process of Ti-5Al-6V alloy. Kim et al. [9] simulated a process, including two subsequent simple shear extrusion and twist extrusion processes and investigated the effect of back pressure and process order. Their results showed that this new combined process can create a more uniform strain in part's cross-section. In 2013, Latypov et al. [10] used simulation to investigate twist extrusion of samples with three different rounded rectangular, fillet rectangular, and elliptical cross-sections. Their results showed that the plastic strain created in all three cross-sections is almost identical, but the force required is

slightly lower for the elliptical cross-section. Elliptical cross-section also resulted in a better part appearance after twist extrusion which can be useful in later passes of the process. Mohammed Iqbal and Senthil Kumar [11] used response surface approach to optimize parameters in the twist extrusion process of AA6082-T6 aluminum alloy. These parameters included force, temperature, and number of passes. Hardness and mechanical strength of parts were used as outputs. Their results showed that a temperature of 500°C and 3 passes leads to optimal results. An increase in the number of passes resulted in 15 to 20% decrease in microstructure size and increase in mechanical properties. Another study regarding twist extrusion and the effect of number of passes on structural uniformity and strain distribution was carried out by Berta et al. [12]. Their results showed heterogeneity in structure, even after 8 passes of twist extrusion and after 8 passes the center of the billet showed less improvement in microstructure compared to the edges. Reshetov et al. [3] in their study investigated the mechanical properties and plastic characteristics of pure titanium under twist extrusion process. They continued the process for 5 passes and their results showed that mechanical properties of the sample reach close to saturation after 2 passes of the process. They also showed that the specimen reaches saturation strain under twist extrusion process faster than HPT process. Bahadori et al. [13] investigated the mechanical properties and microstructures of pure copper under ECAP and twist extrusion processes. Their results showed that samples manufactured using twist extrusion have higher mechanical strength, smaller grain size, and more homogeneous strain. Beygelzimer et al. [14] carried out a theoretical investigation of plastic properties and microstructures of samples under direct extrusion and twist extrusion processes. They concluded that samples undergoing twist extrusion have better properties and that it's better to use the back pressure in twist extrusion process to improve these properties. In another study, Nouri et al. [15] used simulation and empirical tests to investigate the back pressure of the die in twist extrusion by creating a direct extrusion channel in the twist extrusion die. They concluded that the presence of the back pressure results in more homogeneity in plastic strain and increase in mechanical strength of the material.

As can be seen in previous literature, various different studies have investigated twist extrusion process using empirical and simulation methods; however, factors such as cross-section and die angles, which affect the twist extrusion process, have not been investigated in a generalized study. To this end, the current study aims to use three different square, rounded rectangular, and elliptical cross-sections with equal area and different die angles in the twist extrusion process while changing the dimension ratios for elliptical and rectangular dies in order to investigate the effects of these parameters on the plastic strain distribution, microstructure, and deformation forces. Finite element software DEFORM 3D was used for simulations.

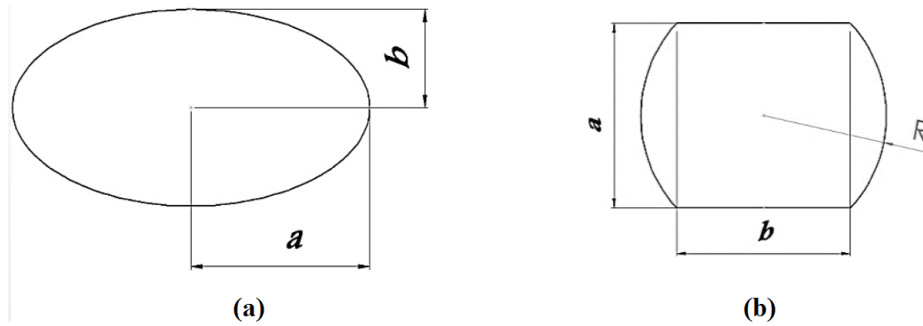


**Fig. 2.** The schematics of cross-sections used for simulation including, a) Elliptical, b) Rounded rectangular.

## 2. Finite Element Simulation

In order to investigate the effect of cross-section on plastic properties and microstructures, three different cross-sections of square, rounded rectangular, and elliptical shape were considered. Sample cross-sections are shown in Fig. 2. Table 1 shows the dimensions used in simulations based on the variables presented in Fig. 2. It is worth noting that the surface dimensions of samples are selected in a way that cross-section area and therefore billet volume is similar in all samples.

**Table 1**  
Dimensions of different cross-sections (in mm).

Cross-section	a (mm)	b (mm)	R (mm)
Elliptical	9	6	-
	10.35	5.2	-
Rounded rectangular	7.9	16.72	9.2
	8.8	15	9.2
Square	13	13	-

Die was designed with three angles ( $\beta$ ). Based on Fig. 1, the die angles used included 20, 37, and 56 degrees. In these simulations, the friction coefficient was equal to 0.01, punch speed of 1.1mm/s, and process temperature was set at 320°C. Based on the element convergence problem, number of elements in the billet were 40400 tetrahedral elements. Fig. 3 shows the schematics of elements of the die and billet.

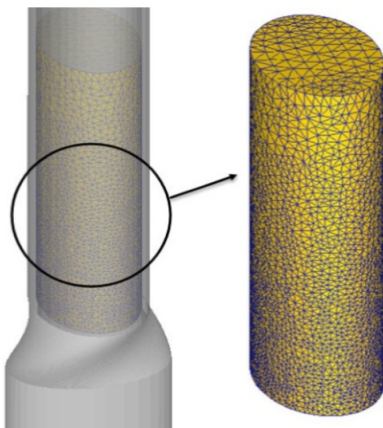


**Fig. 3.** Schematic of part elements and the relevant die.

The Arrhenius equation is widely used to explain the relation between strain rate, flow stress, and temperature at high temperatures. Therefore, this equation was used in the simulations. The Arrhenius equation for Al7050 alloy is presented in Eq. (2) [16].

$$\dot{\varepsilon} = 5.83 \times 10^{18} \left[ \sinh(1.239 \times 10^{-2} \sigma_p) \right]^{7.589} e^{-\frac{2.6406 \times 10^5}{RT}} \quad (1)$$

The dynamic recrystallization mechanism occurs when the dislocation density or strain reach a specific value at high-temperature deformations. Dislocation density and strain value are related to strain rate and process temperature. Various equations are presented for dynamic recrystallization. This simulation used the Avrami recrystallization equations [16].

$$\varepsilon_p = a_1 d_0^{n_1} \dot{\varepsilon}^{m_5} \exp\left(\frac{Q_1}{RT}\right) + C_1 \quad (2)$$

$$X_{DRX} = 1 - \exp\left[-\beta_d \left(\frac{\varepsilon - a_{10}\varepsilon_p}{\varepsilon_{0.5}}\right)^{kd}\right] \quad (3)$$

$$\varepsilon_{0.5} = a_5 d_0^{h_5} \dot{\varepsilon}^{n_5} \dot{\varepsilon}^{m_5} \exp\left(\frac{Q_5}{RT}\right) + C_5 \quad (4)$$

$$d_{DRX} = a_8 d_0^{h_8} \dot{\varepsilon}^{n_8} \dot{\varepsilon}^{m_8} \exp\left(\frac{Q_8}{RT}\right) + C_8 \quad (5)$$

In the above equations,  $\sigma^p$ ,  $\dot{\varepsilon}$ ,  $Q$ ,  $R$ ,  $T$ ,  $X$ ,  $\varepsilon_{0.5}$  and  $d_0$  are peak stress, strain rate, activation energy, universal gas constant, absolute temperature, dynamic recrystallization fraction, strain for 50% recrystallization volume fraction, and initial grain size. The numerical values of the constants in the Avrami recrystallization equations for Al7050 alloy are presented in Table 2.

Before starting the simulations, the accuracy of this work was verified by the results of the research by Nouri et al. [15]. Fig. 4 shows the comparison between this work and ref. [15]. The simulation was done for twist extrusion without BP.

### 3. Results

Fig. 5 shows the contour for accumulated plastic strain and histogram of two extruded samples, one with rounded rectangular cross-section with dimensions of  $15 \times 8.8\text{mm}$  and one with elliptical cross-section with dimensions of  $9 \times 6\text{mm}$  with die angle of  $56$  degree. Furthermore, Table 3 shows the numerical values of accumulated plastic strain for all conditions. In order to eliminate the instability effects of the extruded samples, cross-sections were selected  $10\text{mm}$  after the front surface of the extruded samples.

Fig. 5 shows that the highest plastic strain is observed at the corners and lowest strain occurs in the middle of the samples' cross-section. In the sample with elliptical cross-section, the plastic strain values are high in a larger area of the cross-section which results in a better homogeneity compared to the samples with rounded rectangular cross-section. This can also be confirmed in histogram graphs.

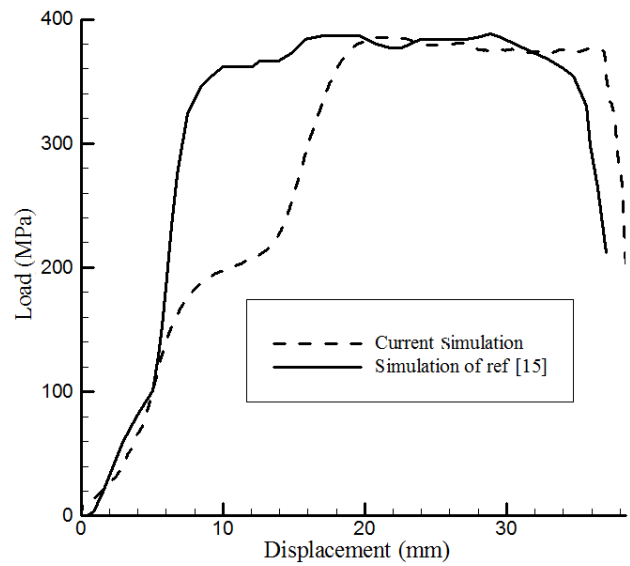
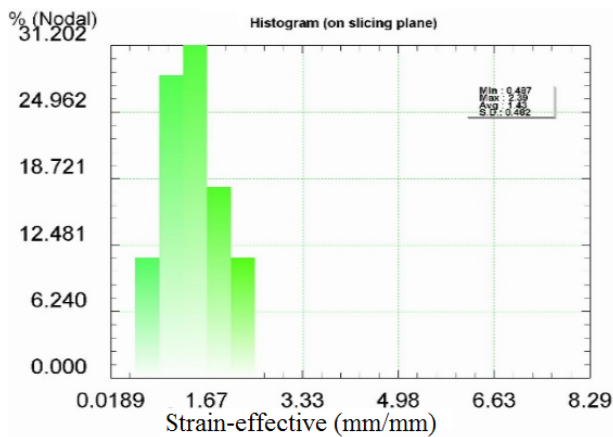


**Fig. 4.** Comparison between the current simulation and ref. [15] (data for twist extrusion without BP).

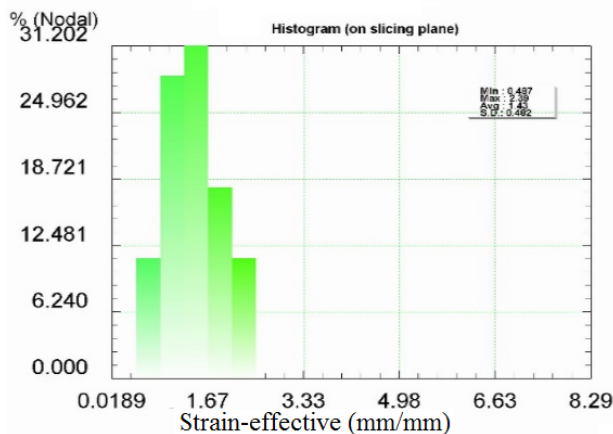
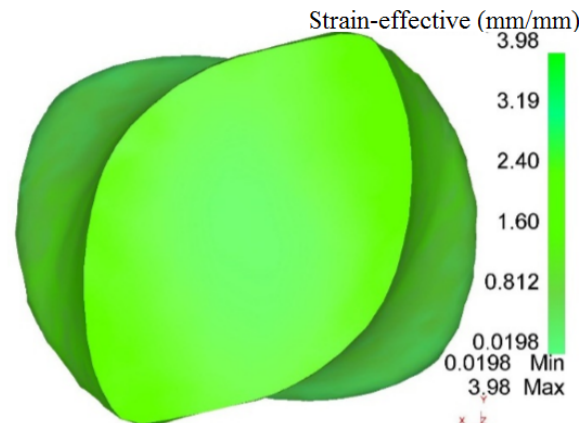
**Table 2**

The values of the Avrami recrystallization equation constants [16].

$\beta_d$	$K_d$	$Q_5$	$Q_8$	$a_5$	$a_8$	$a_{10}$	$h_5$	$m_5$	$m_8$
0.693	2	53350	-19002.72	0.00001214	78.6022	0.8	0.13	0.04	-0.03722



(a)



(b)

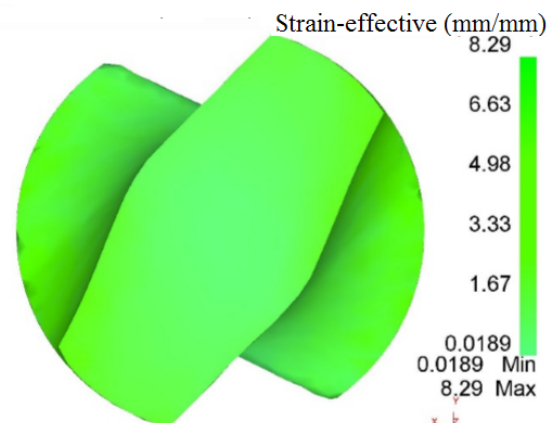


**Fig. 5.** Plastic strain distribution and histogram of extruded samples with die angle of  $56$  degrees, a) Elliptical cross-section of  $9 \times 6\text{mm}$ , b) Rounded rectangular cross-section of  $15 \times 8.8\text{mm}$ .

**Table 3**

The numerical values of accumulated plastic strain under different conditions.

Die angle	Cross section	Minimum strain	Maximum strain	Average strain	Standard deviation
56°	Elliptical 6×9	0.445	2.55	1.21	0.46
	Elliptical 5.2×10.35	0.372	2.15	1.3	0.297
	Rounded rectangular 15×8.8	0.487	2.39	1.43	0.482
	Rounded rectangular 16.72×7.9	0.681	3.84	1.75	0.672
	Square 13×13	0.409	7.6	1.75	1.3
37°	Elliptical 6×9	0.106	1.45	0.53	0.209
	Elliptical 5.2×10.35	0.119	1.12	0.603	0.213
	Rounded rectangular 15×8.8	0.193	1.46	0.711	0.284
	Rounded rectangular 16.72×7.9	0.187	1.99	0.738	0.294
	Square 13×13	0.126	1.96	0.74	0.346
20°	Elliptical 6×9	0.0385	0.305	0.139	0.0542
	Elliptical 5.2×10.35	0.119	1.1	0.599	0.215
	Rounded rectangular 15×8.8	0.0321	0.505	0.183	0.0905
	Rounded rectangular 16.72×7.9	0.0435	0.788	0.228	0.145
	Square 13×13	0.0344	1.99	0.3	0.366

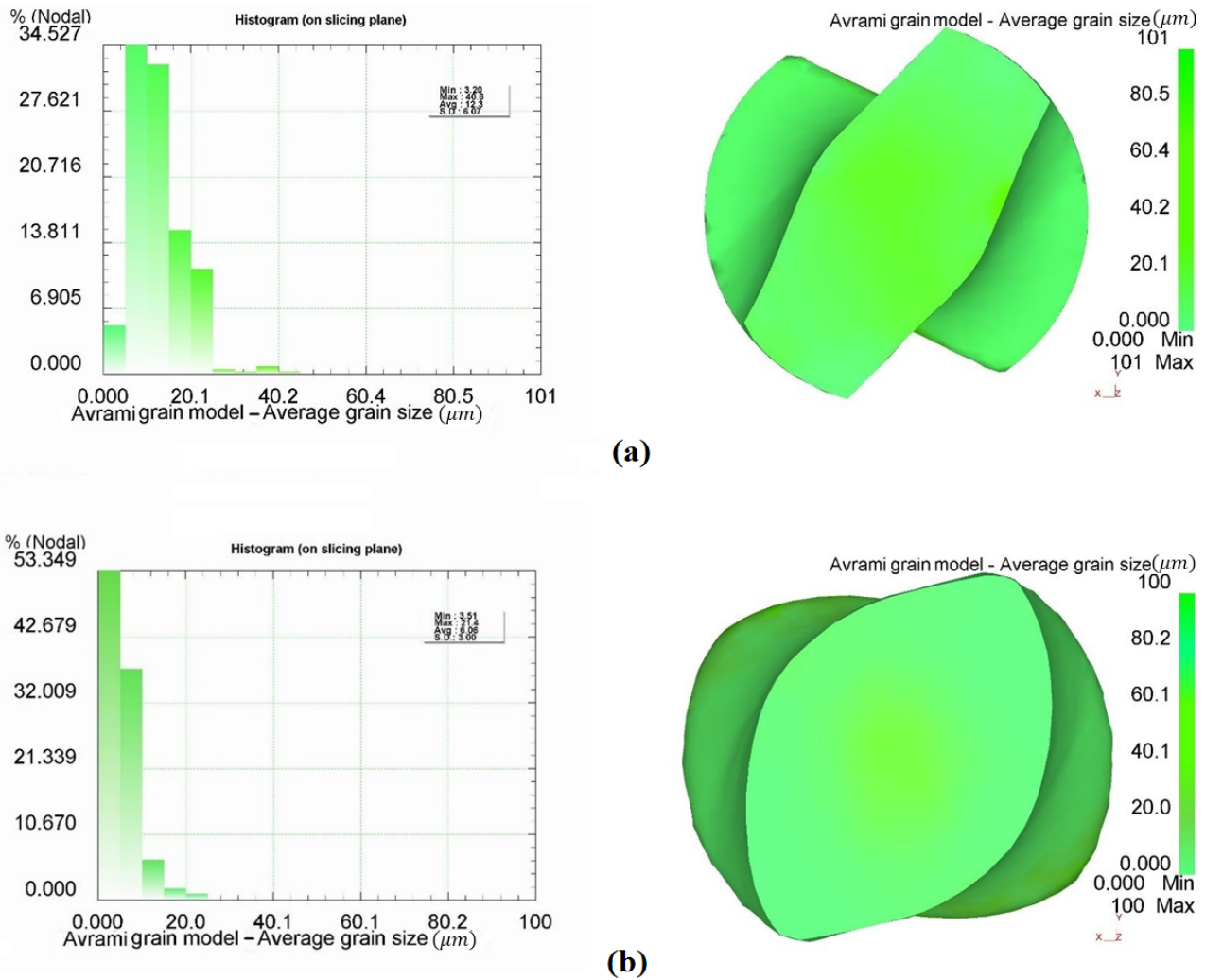
Table 3 shows that plastic strain increases in all cross-sections with increase in die angle. The maximum value for the plastic strain in the square cross-section is higher than the maximum value for other cross-sections. Furthermore, square cross-section has a larger standard deviation compared to other samples which indicates the nonuniform distribution of plastic strain and weaker mechanical properties. This is due to the sharp corners in the square samples. By removing these corners and creating rounded corners, strain decreases. The elliptical cross-section has the lowest average strain compared to other cross sections, but an important factor is the low standard deviation in this cross-section which indicates a more uniform distribution of plastic strain. Suitable uniformity in plastic strain distribution while using elliptical cross-section is also reported in the study by Latypov et al. [10]. As can be seen in the results, in all die angles, changes in the aspect ratio of elliptical and rounded rectangular cross-sections results in changes in plastic strain values. Effect of aspect ratio on the plastic strain is higher in the die angle of 20 degree and decreases with increase in die angle. As can be seen in the die angle of 56 degrees, the effect of aspect ratio for the elliptical cross-section has decreased significantly.

Fig. 6 shows the contour for grain size distribution and histogram of two extruded samples with rounded rectangular cross-section with dimensions of 8.8×15mm and elliptical cross-section with dimensions of 9×6mm, both with die angle of 56 degree. The numerical values of the grain size distribution under different simulation conditions along with details such as standard deviation, average, maximum and minimum grain size values are presented in Table 4. Dynamic recrystallization requires three factors of strain, tem-

perature and strain rate. As can be seen in Fig. 5, the strains created at the center of parts are lower than other areas. This results in larger grain size in the center of samples. As can be seen in Fig. 5, grain size decreases with increase in distance from samples' center. In the sample with elliptical cross-section, it can be seen that the majority of the surface has small grain size, which creates suitable uniformity in grain size, but this is not observed in samples with rounded rectangular which result in higher nonuniformity in grain size distribution.

As can be seen in Table 4, with increase in the die angle, grain size values show a significant decrease. This decrease means that in the die angle of 56 degree, the initial grain size of 100 m in a sample with elliptical 9×6mm cross-section reaches 6.06μm after only one pass of the process. Changes in the cross-section dimensions greatly affect the grain size distribution, but this effect is smaller in rectangular sample. Square samples have the worst results at low die angles while 9×6mm elliptical cross-section shows the best results. This is due to differences in deformation mechanisms. Changes in deformation mechanisms greatly affect microstructures [17]. Based on the standard deviation of grain size distribution, sample with elliptical 9×6mm cross-section shows a very uniform microstructure which is seen in Fig. 5a. This uniformity in grain size distribution greatly affects the mechanical properties of the sample.

Another important factor in the twist extrusion process is the necessary force for deformation. Fig. 6 shows the deformation force for samples with 15×8.8mm rounded rectangular cross-section and 9×6mm elliptical cross-section at die angle of 56 degree.



**Fig. 6.** Grain size distribution and histogram of extruded samples with die angle of 56 degrees and a) Elliptical 9×6mm cross section, b) Rectangular 8.8×15mm cross-section.

**Table 4**

Maximum, minimum and average grain size values and standard deviations under different simulation conditions.

Die angle	Cross section	Minimum strain size ( $\mu\text{m}$ )	Maximum strain size ( $\mu\text{m}$ )	Average strain size ( $\mu\text{m}$ )	Standard deviation size ( $\mu\text{m}$ )
56°	Elliptical 6×9	3.51	21.4	6.6	3
	Elliptical 5.2×10.35	3.98	42.6	14.1	7.71
	Rounded rectangular 15×8.8	3.2	40.6	12.3	6.07
	Rounded rectangular 16.72×7.9	4.92	28.1	13	4.2
	Square 13×13	2.78	28	7.77	4.11
37°	Elliptical 6×9	42.3	100	51.2	9.2
	Elliptical 5.2×10.35	26.6	99.9	65.5	11.08
	Rounded rectangular 15×8.8	43.7	98.8	58.8	12.8
	Rounded rectangular 16.72×7.9	28.5	99.1	82.2	12.1
	Square 13×13	38.6	99.7	85.6	13
20°	Elliptical 6×9	86.9	100	95	0.213
	Elliptical 5.2×10.35	87.1	99.9	96.8	3.37
	Rounded rectangular 15×8.8	95.1	100	96.51	0.312
	Rounded rectangular 16.72×7.9	96.4	100	99.5	0.3
	Square 13×13	100	100	100	-

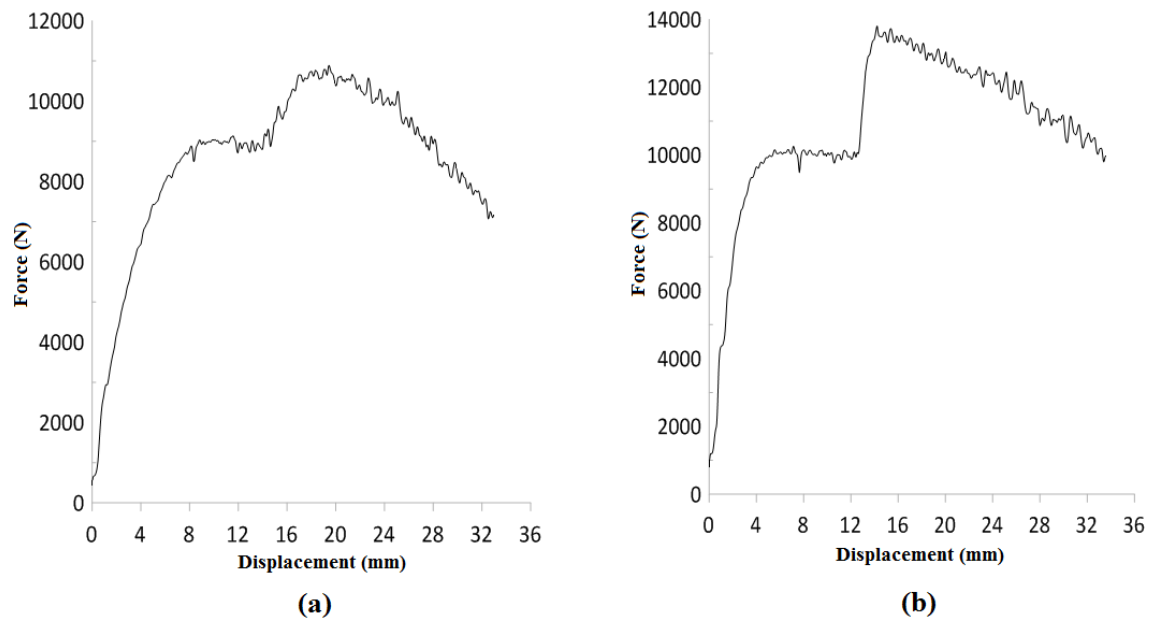


**Fig. 7.** The force applied to the punch for extruded parts at die angle of 56 degree for a) Elliptical  $9 \times 6$ mm cross-section, b) Rectangular  $8.8 \times 15$ mm cross-section.

Table 5 also shows the maximum force values under the different conditions. As can be seen in Fig. 7, there are two increases in the required force in graphs; first is due to the sample entering the starting part of the twist in the die while the second increase is due to the sample reaching the end of the twist part of the die. Based on the force displacement graph, sample with elliptical cross-section has the lowest required force for deformation.

**Table 5**

The maximum force applied to the punch (kN).

Cross section	56°	37°	20°
Elliptical $6 \times 9$	10.9	5.75	2.48
Elliptical $5.2 \times 10.35$	12.4	6.65	2.68
Rounded rectangular $15 \times 8.8$	13.5	8.03	3.2
Rounded rectangular $16.72 \times 7.9$	13.2	7.36	2.91
Square $13 \times 13$	14.2	8.96	4.12

The maximum values presented in Table 5 show that increase in the die angle results in an increase in deformation force. Furthermore, changes in the dimensions of rounded rectangular sample don't significantly affect the required force, but dimension changes in the elliptical part significantly change in the force required for deformation; smaller aspect ratios requiring lower force. Maximum force required for deformation belongs to the sample with square cross-section which is due to presence of sharp corners and twisting method of this sample inside the die.

#### 4. Conclusions

This article investigated the effects of extrusion die angle, shape and aspect ratio of billet cross-section on

plastic strain distribution and microstructures of Aluminum Al7050 alloy with initial grain size of 100 m using simulation in DEFORM 3D software. The most important conclusions based on the results of the current study are as follows:

1. Increase in die angle results in improving material's microstructures.
2. Using rounded rectangular cross-section can be as effective as using elliptical cross-section on changing microstructures.
3. Strain distribution is more uniform in samples with elliptical cross-section.
4. Evaluating the simulation results showed that in all cases, using elliptical cross-section is effective in reducing the required punch force and this effect is more prominent at die angle of 56 degree.
5. In constant cross-section area, the elliptical-shaped sample with dimensions of  $9 \times 6$ mm, which has the lowest aspect ratio, showed the best microstructure based on grain size and distribution. This sample also required the lowest amount of force for deformation.

#### References

- [1] Y. Estrin, S.B. Yi, H.G. Brokmeier, Z. Zúberová, S.C. Yoon, H.S. Kim, R.J. Hellmig, Microstructure, texture and mechanical properties of the magnesium alloy AZ31 processed by ECAP, *Int. J. Mater. Res.*, 99(1) (2008) 50-55.

- [2] J. Nemati, S. Sulaiman, A. Khalkhali, Improvement in mechanical properties of Titanium deformed by ECAE process, *J. Stress Anal.*, 1(1) (2016) 55-64.
- [3] A. Reshetov, R. Kulagin, A. Korshunov, Y. Beygelzimer, The occurrence of ideal plastic state in CP titanium processed by twist extrusion, *Adv. Eng. Mater.*, 20(5) (2018) 1700899.
- [4] A. Alavi Nia, S.H. Nourbakhsh, Microstructure and Mechanical Properties of AZ31/SiC and AZ31/CNT Composites Produced by Friction Stir Processing, *Trans. Indian Inst. Met.*, 69(7) (2016) 1435-1442.
- [5] F. Javadzadeh Kalahroudi, H. Koohdar, H.R. Jafarian, Y. Haung, T.G. Langdon, M. Nili-Ahmadabadi, On the microstructure and mechanical properties of an Fe-10Ni-7Mn martensitic steel processed by high-pressure torsion, *Mater. Sci. Eng. A*, 749 (2019) 27-34.
- [6] Y. Beygelzimer, A. Reshetov, S. Synkov, O. Prokof'eva, R. Kulagin, Kinematics of metal flow during twist extrusion investigated with a new experimental method, *J. Mater. Process. Technol.*, 209(7) (2009) 3650-3656.
- [7] M. Jahedi, M.H. Paydar, Three-dimensional finite element analysis of torsion extrusion (TE) as an SPD process, *Mater. Sci. Eng. A*, 528(29-30) (2011) 8742-8749.
- [8] S.A.A. Akbari Mousavi, A.R. Shahab, M. Mastroori, Computational study of Ti-6Al-4V flow behaviors during the twist extrusion process, *Mater. Des.*, 29(7) (2008) 1316-1329.
- [9] J.G. Kim, M. Latypov, N. Pardis, Y.E. Beygelzimer, H.S. Kim, Finite element analysis of the plastic deformation in tandem process of simple shear extrusion and twist extrusion, *Mater. Des.*, 83 (2015) 858-865.
- [10] M.I. Latypov, Y. Beygelzimer, H.S. Kim, Comparative analysis of two twist-based SPD processes: Elliptical cross-section spiral equal-channel extrusion vs. Twist Extrusion, *Mater. Trans.*, 54(9) (2013) 1587-1591.
- [11] U. Mohammed Iqbal, V. Senthil Kumar, Modeling of twist extrusion process parameters of AA6082-T6 alloy by response surface approach, *Proc. Inst. Mech. Eng. B. J. Eng. Manuf.*, 228(11) (2014) 1458-1468.
- [12] M. Berta, D. Orlov, P.B. Prangnell, Grain refinement response during twist extrusion of an Al-0.13% Mg alloy, *Int. J. Mater. Res.*, 98(3) (2007) 200-204.
- [13] S.R. Bahadori, K. Dehghani, S.A.A. Akbari Mousavi, Comparison of microstructure and mechanical properties of pure copper processed by twist extrusion and equal channel angular pressing, *Mater. Lett.*, 152 (2015) 48-52.
- [14] Y.E. Beygelzimer, O.V. Prokof'eva, V.N. Varyukhin, Structural changes in metals subjected to direct or twist extrusion: Mathematical simulation, *Russ. Metall.*, 2006(1) (2006) 25-32.
- [15] M. Nouri, H.R. Mohammadian Semnani, E. Emadoddin, H.S. Kim, Investigation of direct extrusion channel effects on twist extrusion using experimental and finite element analysis, *Measurement*, 127 (2018) 115-123.
- [16] Y.P. Yi, X. Fu, J.D. Cui, H. Chen, Prediction of grain size for large-sized aluminium alloy 7050 forging during hot forming, *J. Cent. South Univ. Technol.*, 15(1) (2008) 1-5.
- [17] V.M. Segal, Severe plastic deformation: simple shear versus pure shear, *Mater. Sci. Eng. A*, 338(1) (2002) 331-344.